arXiv:1202.0782v1 [math.DG] 3 Feb 2012

The Jacobian of a Riemann surface and the geometry of the cut locus of simple closed geodesics

Muetzel, Bjoern*

Department of Mathematics, Université Montpellier 2, place Eugène Bataillon,
34095 Montpellier cedex 5, France

February 6, 2012

Abstract

To any compact Riemann surface of genus g one may assign a principally polarized abelian variety of dimension g, the *Jacobian* of the Riemann surface. The Jacobian is a complex torus and we call a Gram matrix of the lattice of a Jacobian a *period Gram matrix*. We give upper and lower bounds for all entries of the period Gram matrix with respect to a suitable homology basis. These bounds depend on the geometry of the cut locus of non-separating simple closed geodesics (scg). We first present a theoretical approach that relies on the premise that these cut loci can be calculated. Then we give an example where our upper bound is sharp. Finally we give practical estimates based on the geometry of Q-pieces that contain a canonical homology basis. The methods developed here have been applied to surfaces that contain small non-separating scgs in [BMMS].

Mathematics Subject Classifications: 14H40, 14H42, 30F15 and 30F45.

1 Introduction

Let S be a hyperbolic Riemann surface of genus $g \geq 2$ and let $\mathrm{A} = (\alpha_i)_{i=1\ldots 2g}$ be a *canonical homology basis* of closed cycles on the surface. This basis is assumed to be given in the following way:

$$\mathrm{A} = (\alpha_1, \alpha_{\tau(1)}, ..., \alpha_g, \alpha_{\tau(g)}).$$

Here each α_i is a simple closed curve and the curves are paired, such that for each α_i there exists exactly one $\alpha_{\tau(i)} \in (\alpha_j)_{j=1\ldots 2g}$ that intersects α_i in exactly one point and there are no other intersection points. In the vector space of real harmonic forms on S let $(\sigma_k)_{k=1\ldots 2g}$ be a *dual basis for* $(\alpha_i)_{i=1\ldots 2g}$ defined by

$$\int_{\alpha_i} \sigma_k = \delta_{ik}.$$

The *period Gram matrix* Q_S of a compact Riemann surface (R.S.) S of genus g is the Gram matrix

---

[*] E-mail address : bjorn.mutzel@gmail.com

$$Q_S = (\langle \sigma_i, \sigma_j \rangle)_{i,j=1\dots 2g} = \left(\int_S \sigma_i \wedge {}^*\sigma_j \right)_{i,j=1\dots 2g}$$

This period matrix Q_S defines a complex torus, the *Jacobian* or *Jacobian variety* $J(S)$ of the Riemann surface S (see [FK], chapter III). We denote by

$$E(\sigma_i) = E_S(\sigma_i) = \int_S \sigma_i \wedge {}^*\sigma_i = \langle \sigma_i, \sigma_i \rangle$$

the *energy of* σ_i *(over* S*).* As Q_S is a Gram matrix $E(\sigma_i)$ is also the squared norm of a vector v_i in the lattice of the Jacobian. By Riemann's period relations the Jacobian is a principally polarized abelian variety (PPAV) (see [BL], section 4.1 for a definition). The lattices of PPAVs are exactly the symplectic lattices ([BS]). The Schottky problem is to characterize the Jacobians among the PPAVs.

Buser and Sarnak ([BS]) approached this problem by means of a geometric invariant, the squared norm of the shortest non-zero vector, in the lattice of a Jacobian of a Riemann surface of genus g is bounded from above by $\log(4g)$, whereas it can be of order g for the lattice of a PPAV of dimension g. More insight has been obtained recently into the connection between the global geometry of a compact Riemann surface of genus g and the geometry of its Jacobian. The $\log(g)$-bound on the squared norm of a lattice vector of the Jacobian has been further extended in [BPS] to almost g linear independent vectors. In [Mu3] it was shown that in the case of a hyperelliptic surface the squared length of the shortest lattice vector is bounded from above by a constant independent of the genus.

In this article we examine the connection between the concrete geometry of a compact Riemann surface and the geometry of its Jacobian. This approach has been taken in special cases, for example when the Riemann surface is a real algebraic curve. Here algorithms exist to calculate the period matrix (see [BSi], [Hi] or [Se]), but these methods are limited to these cases. Though the estimates obtained in this article are not sharp in general, the methods apply to any Riemann surface.

Here we give upper and lower bounds for all entries of the period Gram matrix given with respect to a canonical homology basis. To this end we have to estimate the energy of the dual harmonic forms on the surface. We find upper bounds for the energy of these forms by estimating the capacity of hyperbolic tubes. The boundary of such a tube is provided by the cut locus of a cycle in the homology basis or a related scg. We then use projections of vector fields onto curves to obtain a lower bound. This theoretical approach relies on the premise that these cut loci can be calculated. We furthermore provide two examples for our approach. One that shows the limitations of the method and one where the upper bound is sharp. Finally we present practical estimates based on the geometry of surfaces of signature $(1, 1)$, or Q-pieces, containing the paired curves of the homology basis. Under this condition the cut loci can be - at least partially - calculated. The methods developed here have been applied to surfaces that contain small scgs in [BMMS]. In this case more refined estimates are obtained.

This article is structured in the following way. We will first introduce the necessary tools and definitions in section 2. Then we present the theoretical approach in section 3. Finally we provide practical upper and lower bounds based on the geometry of Q-pieces in section 4.

2 Preliminaries

Many calculations presented in the following sections rely on the embedding of topological tubes around scgs of Riemann surfaces into hyperbolic cylinders and subsequent approximations and calculations in Fermi coordinates. We will present all these concepts in this section.

The Poincare model of the hyperbolic plane is the following subset of the complex plane $\mathbb{C}$:

$$\mathbb{H} = \{z = x + iy \in \mathbb{C} \mid y > 0\}$$

with the hyperbolic metric

$$ds^2 = \frac{1}{y^2}(dx^2 + dy^2).$$

Fermi coordinates ψ_η *with baseline* η *and base point* p are defined in the following way. The Fermi coordinates are a bijective parametrization of $\mathbb{H}$

$$\psi_\eta : \mathbb{R}^2 \to \mathbb{H}, \psi_\eta : (t, s) \mapsto \psi_\eta(t, s),$$

where $\psi_\eta(0, 0) = p$. Each point $q = \psi_\eta(t, s) \in \mathbb{H}$ can be reached in the following way. Starting from the base point p we first move along η the directed distance t to $\psi_\eta(t, 0)$. There is a unique geodesic, ν, intersecting η perpendicularly in $\psi_\eta(t, 0)$. From $\psi_\eta(t, 0)$ we now move along ν the directed distance s to $\psi_\eta(t, s)$.
The parametrization $\psi : \mathbb{R}^2 \to \mathbb{H}$

$$\psi(t, s) := \frac{\exp(t)}{\cosh(s)}(\sinh(s) + i)$$

are the Fermi coordinates with baseline $\{iy \mid y \in \mathbb{R}_+\}$ and base point i. Fermi coordinates for any geodesic in $\mathbb{H}$ can be obtained by conjugation of $\psi(t, s)$ with the suitable isometries.
A *hyperbolic cylinder* C or shortly *cylinder* is a set that is isometric to the set

$$\{\psi(t, s) \mid (t, s) \in [0, a] \times [b_1, b_2]\} \mod \{\psi(0, s) = \psi(a, s) \mid s \in [b_1, b_2]\},$$

with the induced metric from $\mathbb{H}$. The baseline of C is the shortest scg in C of length a.
Consider a cylinder C. Let $A \subset C$ be a set and $F \in \mathrm{Lip}(\bar{A})$ a Lipschitz function on the closure of A. Let G be the metric tensor with respect to the Fermi coordinates. Then the *energy of* F *on* A, $E_A(F)$ is given by

$$E_A(F) = \iint\limits_{\psi^{-1}(A)} \|D(F \circ \psi)\|^2_{G^{-1}} \sqrt{\det(G)}.$$

Using Fermi coordinates, we obtain for the energy of F on A, $E_A(F)$, with $F \circ \psi = f$:

$$E_A(F) = \iint\limits_{\psi^{-1}(A)} \frac{1}{\cosh(s)} \frac{\partial f(t, s)}{\partial t}^2 + \cosh(s) \frac{\partial f(t, s)}{\partial s}^2 \, ds \, dt \geq \iint\limits_{\psi^{-1}(A)} \cosh(s) \frac{\partial f(t, s)}{\partial s}^2 \qquad (1)$$

The *capacity* of an annulus $A \subset C$, $\mathrm{cap}(A)$ is given by

$$\mathrm{cap}(A) = \inf\{E_A(F) \mid \{F \in \mathrm{Lip}(\bar{A}) \mid F|_{\partial_1(A)} = 0, F|_{\partial_2(A)} = 1\}\}.$$

Let S be a compact R.S. and $(\alpha_i)_{i=1\dots 2g}$ a canonical homology basis on S. The *collar* $C(\eta)$ of a simple closed geodesic η, is defined by

$$C(\eta) = \{x \in S \mid \operatorname{dist}(x, \eta) < w\}.$$

Here w is the supremum of all ω, such that the geodesic arcs of length ω emanating perpendicularly from η are pairwise disjoint. The closure $\overline{C(\eta)}$ of a collar is a cylinder of constant width. For a given α_i, $\alpha_{\tau(i)}$ is the unique scg in the canonical homology basis that intersects α_i. In [Mu3] it was shown that the capacity of any cylinder C' with baseline $\alpha_{\tau(i)}$ contained in $C(\alpha_{\tau(i)})$ provides an upper bound for the energy $E(\sigma_i)$ of the dual harmonic form σ_i. If $w_{\tau(i)}$ is the width of $C(\alpha_{\tau(i)})$, then

$$E(\sigma_i) = \int_S \sigma_i \wedge {}^*\sigma_i < \frac{l(\alpha_{\tau(i)})}{\pi - 2\arcsin\left(\frac{1}{\cosh(w_{\tau(i)})}\right)} = \operatorname{cap}(C(\alpha_{\tau(i)})) \leq \operatorname{cap}(C'). \tag{2}$$

It is noteworthy that we can deduce this inequality by finding the minimal function for the capacity problem. We obtain this function by solving the Euler-Lagrange equation (see [Ge] p. 152-154) applied to equation (1). For a more detailed account see [Mu1], p. 23-27.

3 Theoretical estimates for the period Gram matrix

Let S be a Riemann surface of genus g and A a canonical homology basis. Let Q_S be the period Gram matrix of S with respect to A,

$$Q_S = (q_{ij})_{i,j=1\dots 2g} = \left(\int_S \sigma_i \wedge {}^*\sigma_j\right)_{i,j=1\dots 2g}.$$

From equation (2) we obtain an upper bound on the diagonal entries of Q_S by evaluating the capacity of a cylinder around the elements of the canonical homology basis. This approach can be expanded to obtain better estimates of these entries and finally of all entries of Q_S. The approach relies on the premise that the cut locus of a given simple closed geodesic on a Riemann surface can be - at least partially - calculated.

3.1 Estimates for the diagonal entries of Q_S

We first show how to obtain upper and lower bounds on the diagonal entries of Q_S. Consider WLOG $E(\sigma_1) = q_{11}$. Let $T(\alpha_2) \subset S$ be a topological tube which is obtained by a continuous deformation of the collar $C(\alpha_2)$ in S. Using the same arguments that are used in [BS], p. 36 for hyperbolic cylinders, we see that the capacity of such a tube $T(\alpha_2)$ gives an upper bound for the energy of σ_1, $E(\sigma_1)$:

$$E(\sigma_1) \leq \operatorname{cap}(T(\alpha_2)).$$

We will use the tube that we obtain by cutting open S along the cut locus $CL(\alpha_2)$ of α_2. The *cut locus* of a subset $X \subset S$, $CL(X)$ is defined in the following way, where $\gamma_{a,b}$ denotes a geodesic arc connecting the points a and b:

$$CL(X) := \{y \in S \mid \exists \gamma_{x,y}, \gamma_{x',y}, \gamma_{x,y} \neq \gamma_{x',y}, \text{ with } x, x' \in X \text{ and } \operatorname{dist}(x,y) = l(\gamma_{x,y}) = l(\gamma_{x',y})\}.$$

For more information about the cut locus, see [Ba]. We denote by S_X the surface, which we obtain by cutting open S along $CL(X)$. For a set $X \subset S$, set

$$Z_r(X) = \{x \in S \mid \operatorname{dist}(x, X) \leq r\}.$$

Let U be a set of disjoint simple closed geodesics $(\gamma_i)_{i=1,\dots,n}$ then for sufficiently small r, $Z_r(U)$ consists of disjoint cylinders around these geodesics. We obtain $CL(U)$ by letting r grow continuously until $Z_r(U)$ self-intersects. We stop the expansion in the points of intersection, but continue expanding the rest of the set, until the process halts. The points of intersection then form $CL(U)$. It follows from this process that the surface S_U, which we obtain by cutting open S along $CL(U)$ can be retracted onto the union of small cylinders around the $(\gamma_i)_{i=1,\dots,n}$. If $U = \gamma$, then S_U can be embedded into an sufficiently large cylinder C around γ.
Consider an embedding of $S_{\alpha_2} = S_2$ in a cylinder C, which, by abuse of notation, we also call S_2. This is shown in *Figure 1*. The boundary ∂S_2 of $S_2 \subset C$ consists of the two connected components $\partial_1 S_2$ and $\partial_2 S_2$, which are piecewise geodesic (see [Ba]). Fixing a base point $x \in S_2 \subset C$,

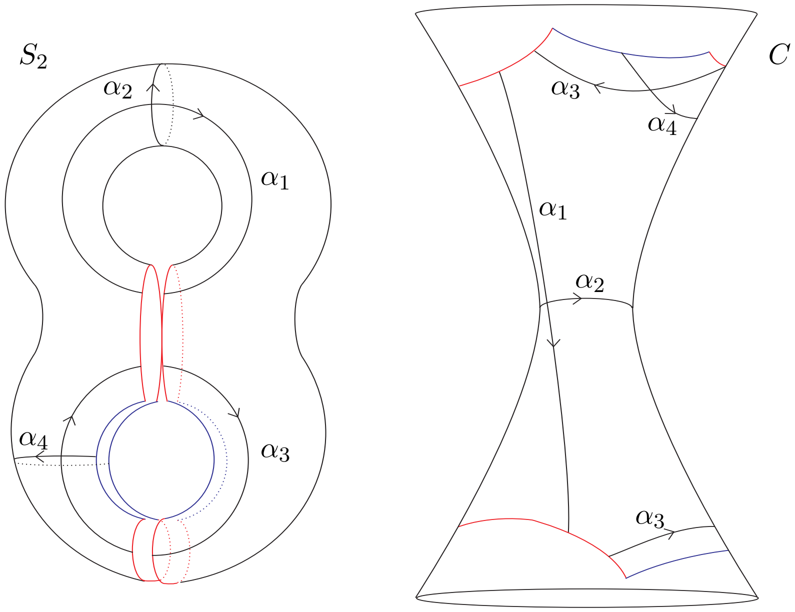

Figure 1: Embedding of $S_2 = S_{\alpha_2}$ in a cylinder around α_2 .

we can construct a primitive F_1 of σ_1 by integrating σ_1 along paths starting from the base point x. As $\int\limits_{\alpha_2} \sigma_1 = 0$, the value of the integral is independent of the chosen path in S_2. Therefore there exists a primitive F_1 of σ_1 on $S_2 \subset C$. Furthermore F_1 is a real harmonic function, as σ_1 is a real harmonic 1-form. We remind here that the value of the integral of a σ_1 over a closed curve depends only on the homology class of the curve. Especially the value of the integral is the same for two curves in the same free homotopy class.
The conditions on the homology basis A imply the following boundary conditions for F_1. For each point p_1 on the boundary $\partial S_2 \subset C$, there exists a point p_2 that maps to the same point p on S as p_1, such that

$$F_1(p_2) - F_1(p_1) = 0 \quad \text{or} \quad F_1(p_2) - F_1(p_1) = 1.$$

We color p_1 and p_2 blue in the first case and red in the second case and call such a decomposition a *red-blue decomposition* of the cut locus. Such a decomposition is shown in *Figure 1.*
We denote by $CL^{blue}(\alpha_2)$ and $CL^{red}(\alpha_2)$ the blue and red parts of $CL(\alpha_2)$, both in S and S_2. We have that

$$CL(\alpha_2) = CL^{blue}(\alpha_2) \cup CL^{red}(\alpha_2).$$

For the red-blue decomposition that is obtained via the cut locus $CL(\alpha_2)$, the following holds. If p_1 and p_2 are blue, then p_1 and p_2 lie on the same side of the boundary ∂S_2. If p_1 and p_2 are red then they lie on different sides of ∂S_2. This follows from the relationship of the canonical 1-forms with the intersection number of curves (see [FK], chapter III). There are points on ∂S_2 that are both red and blue. However the number of those points is finite.
We now connect the endpoints of two corresponding opposite red boundary segments in the red-blue composition of $S_2 \subset C$ with differentiable curves, such that these curves do not mutually intersect. Then the curves, together with the boundary segments of S_2, enclose a subset of S_2. We denote the union of all enclosed areas that can be obtained in this way by S_2^{red}. We set:

$$S_2^{blue} = S_2 \backslash S_2^{red}, \text{ therefore } S_2 = S_2^{red} \cup S_2^{blue}.$$

We also call such a decomposition of S_2 a *red-blue decompositon.* Note that the connected red and blue parts on each boundary of $CL(\alpha_2)$ alternate and that the boundaries of S_2^{blue} contain the blue parts of $CL(\alpha_2)$. By construction of S_2^{red}, the red and blue parts of S_2 do also alternate. The connected subsets of $CL^{blue}(\alpha_2)$ are paired via the red-blue decomposition. This induces a pairing of the connected areas of S_2^{blue}. Two such pairs are isometric.

Upper bound

The capacity of $S_2 \subset C$, $\operatorname{cap}(S_2)$ provides an upper bound on the energy of σ_1. We obtain an upper bound on $\operatorname{cap}(S_2)$ by evaluating the energy of any test function F_{1t}, which is a Lipschitz function on S_2 and satisfies the boundary conditions of the capacity problem (see [GT]):

$$E(F_{1t}) \geq \operatorname{cap}(S_2) \geq E(\sigma_1) = q_{11}.$$

In [Mu2] **Theorem 4.2.** we obtain general upper and lower bounds on the capacity of annuli A on a cylinder of constant curvature. Here an annulus is a region that can be obtained by a continuous deformation of the cylinder itself. The idea for the upper bound is to construct a test function in the following way. We adapt the harmonic function that solves the capacity problem for cylinders of constant width (see (2)) to the boundary using the parametrization of a cylinder in Fermi coordinates. If the annulus $A \subset C$ is given in Fermi coordinates by

$$A = \psi\{(t,s) \mid s \in [a_1(t), a_2(t)], t \in [0, l(\alpha_2)]\},$$

where $a_1(\cdot)$ and $a_2(\cdot)$ are piecewise differentiable functions with respect to t, then it follows:

Theorem 3.1 *There exists a Lipschitz function* $\tilde{F} \in \operatorname{Lip}(A)$*, such that for* $H(s) = 2\arctan(\exp(s))$ *and* $q_i(t) = \frac{\partial H(s_0)}{\partial s}|_{s_0 = a_i(t)} \cdot a_i'(t)$ *for* $i \in \{1,2\}$*, we have:*

$$\int\limits_0^{l(\alpha_2)} \frac{1 + \frac{q_1(t)^2 + q_1(t)q_2(t) + q_2(t)^2}{3}}{H(a_2(t)) - H(a_1(t))}\, dt = E(\tilde{F}) \geq \operatorname{cap}(A) \geq \int\limits_0^{l(\alpha_2)} \frac{1}{H(a_2(t)) - H(a_1(t))}\, dt$$

As $S_2 \subset C$ is an annulus that satisfies the conditions of **Theorem 3.1**, we can apply this theorem to obtain an estimate of the capacity $\operatorname{cap}(S_2)$. It is noteworthy that the lower bound is obtained by finding the optimal function that minimizes the last integral in equation (1). This integral is equal to the energy of the projection of the gradient of a function. Here the gradient is projected onto the geodesics intersecting the baseline of C perpendicularly.
We now shortly describe a further modification that should lead to an improved upper bound. Though we have not applied this modification in our practical estimates, we think that it leads to a test function F_{1t} that is close to the harmonic function F_1. This modification can be applied if a connected subset S^b of S_2^{blue} is large. On the boundary $\partial_1 S^b$, where our test function F_{1t} equals 1, we move along the boundary line and decrease the boundary values until they reach $\frac{1}{2}$. After a plateau, where the boundary values are constant we increase the values in the same fashion when towards the other end of $\partial_1 S^b$. On the opposite boundary $\partial_2 S^b$, we do the opposite. First we increase the values to $\frac{1}{2}$. After a plateau we decrease the boundary values again to 0. There is a paired subset S'^b of S_2^{blue} isometric to S^b. Transplanting F_{1t} from S^b via the isometry onto S'^b, we obtain a function F_{1t} that satisfies the boundary conditions induced by the red-blue decompositon of F_1. However, in this case we have to assure that the 1-form dF_{1t} extends to a closed 1-form on S. If this condition is satisfied, we have $E(F_{1t}) \geq E(\sigma_1)$ due to the energy minimizing property of σ_1. The energy $E(F_{1t})$ of our new test function should provide a better upper bound for $E(\sigma_1)$ than $\operatorname{cap}(S_2)$.

Lower bound

We obtain a lower bound on $q_{11} = E(F_1)$ in the following way. Consider the set S_2^{red}. Remember that in each connected subset of S_2^{red} there are boundary points p_1 and p_2 on opposite sides, such that $F_1(p_2) - F_1(p_1) = 1$. We have:

$$E(\sigma_1) = E(F_1) \geq \int\limits_{S_2^{red}} \|DF_1\|_2^2.$$

Let I be a disjoint union of intervals in $\mathbb{R}$ and

$$\varphi : I \times [a_1, a_2] \to S_2^{red}, \varphi : (t, s) \mapsto \varphi(t, s)$$

a bijective function that parametrizes S_2^{red} in the following way:

$$\varphi(I \times \{a_1\}) = S_2^{red} \cap \partial_1 S_2 \quad \text{and} \quad \varphi(I \times \{a_2\}) = S_2^{red} \cap \partial_2 S_2$$

and for a fixed $c \in I$, $\varphi(\{c\} \times [a_1, a_2])$ is a differentiable curve in S_2^{red}, such that

$$F_1(\varphi(c, a_2)) - F_1(\varphi(c, a_1)) = 1.$$

Denote by $\mathcal{F}_1$ the set of functions

$$\mathcal{F}_1 = \{f : S_2^{red} \to \mathbb{R} \mid f \in \operatorname{Lip}(S_2^{red}) \ \text{ and } \ f(\varphi(c, a_2)) - f(\varphi(c, a_1)) = 1 \ \ \forall \ \ c \in I\}.$$

We obtain a lower bound on $q_{11} = E(\sigma_1) = E(F_1)$ if we can find a function $\tilde{f}_1$, such that

$$\int\limits_{S_2^{red}} \|D\tilde{f}_1\|_2^2 = \min_{f \in \mathcal{F}_1} \int\limits_{S_2^{red}} \|Df\|_2^2. \tag{3}$$

We call this problem the *free boundary problem* for S_2^{red}.
Though this problem is quite interesting in its own right, we could not find an explicit solution. To obtain an explicit result, we construct another lower bound based on projection of tangent vectors onto curves. For a $x = \varphi(c,a) \in S_2^{red}$ denote by $p_\varphi : T_x(S_2^{red}) \to \{\lambda \cdot \frac{\partial\varphi(c,a)}{\partial s} \mid \lambda \in \mathbb{R}\}$ the orthogonal projection of a tangent vector in x onto the subspace spanned by $\frac{\partial\varphi(c,a)}{\partial s}$. Then we have:

$$E(F_1) \geq \int\limits_{S_2^{red}} \|DF_1\|_2^2 \geq \int\limits_{S_2^{red}} \|p_\varphi(DF_1)\|_2^2 \geq \min_{f\in\mathcal{F}_1} \int\limits_{S_2^{red}} \|p_\varphi(Df)\|_2^2 = \int\limits_{S_2^{red}} \|p_\varphi(Df_1)\|_2^2. \tag{4}$$

Here f_1 is a function that realizes the minimum. We have $\int\limits_{S_2^{red}} \|DF_1\|_2^2 = \int\limits_{S_2^{red}} \|p_\varphi(DF_1)\|_2^2$, if and only if in every point $\varphi(t,s) = x \in S_2^{red}, \varphi(t,\cdot)$ is orthogonal to the level set of F_1 passing through x. Note that the problem of finding the function f_1 is in general easier than finding the function F_1 or $\tilde{f}_1$. We will apply these ideas to Q-pieces in the following section. To this end we will use results from the calculus of variations.
In total we have the following estimates for $q_{11} = E(\sigma_1)$:

$$\mathrm{cap}(S_{\alpha_2}) \geq E(\sigma_1) = E(F_1) \geq \min_{f\in\mathcal{F}_1} \int\limits_{S_2^{red}} \|Df\|_2^2 \geq \min_{f\in\mathcal{F}_1} \int\limits_{S_2^{red}} \|p_\varphi(Df)\|_2^2.$$

If the geometry of the cut locus $CL(\alpha_2)$ is known, we obtain an explicit estimate for $\mathrm{cap}(S_{\alpha_2})$ from **Theorem 3.1**.
Note that the test function whose energy provides our upper bound has positive energy on S_2^{blue}, whereas the energy is zero on S_2^{blue} in the estimate providing the lower bound. This is one reasons why the upper bound differs from the lower bound. Another difference is due to the use of the projection along lines in the construction of the lower bound. In section 4, we will apply these methods to a decomposition of the Riemann surface, where the elements of the canonical homology basis are contained in Q-pieces. Here we will see these two effects explicitely.

3.2 Estimates for the non-diagonal entries of Q_S

We now show, how we can estimate the remaining entries of the period Gram matrix Q_S. For $i \neq j$, we have, as $\int\limits_S \cdot \wedge {}^*\cdot$ is a scalar product:

$$\begin{aligned} |q_{ij}| &\leq \frac{1}{2}\left(E(\sigma_i) + E(\sigma_j)\right), & (5)\\ q_{ij} &= \frac{1}{2}\left(E(\sigma_i+\sigma_j) - E(\sigma_i) - E(\sigma_j)\right) \quad \text{and} & (6)\\ q_{ij} &= \frac{1}{2}\left(E(\sigma_i) + E(\sigma_j) - E(\sigma_i-\sigma_j)\right). & (7)\end{aligned}$$

We have shown how to find upper and lower bounds on $E(\sigma_i)$ and $E(\sigma_j)$. We obtain a direct estimate on q_{ij} from equation (5). However to obtain a sharp estimate, both $E(\sigma_i)$ and $E(\sigma_j)$ must be small. We will show how to obtain better estimates for q_{ij} from the following two equations. Here we obtain an estimate for q_{ij}, if we can find upper and lower bounds on either

$E(\sigma_i+\sigma_j)$ or $E(\sigma_i-\sigma_j)$.
Consider the harmonic 1-forms ω_1 and ω_2 that satisfy the following equations on the cycles:

$$\int\limits_{\alpha_k}\omega_1 \quad = \quad \delta_{ik}+\delta_{jk} \quad \text{for all} \quad k\in\{1,..,2g\}. \tag{8}$$

$$\int\limits_{\alpha_k}\omega_2 \quad = \quad \delta_{ik}-\delta_{jk} \quad \text{for all} \quad k\in\{1,..,2g\}. \tag{9}$$

It follows easily from the uniqueness of the harmonic 1-form that satisfies these integral conditions that $\sigma_i+\sigma_j$ is the unique 1-form that minimizes the energy among all closed 1-forms that satisfy equation (8) and that $\sigma_i-\sigma_j$ is the unique 1-form that minimizes the energy among all closed 1-forms that satisfy equation (9).
There is a geodesic α in the homotopy class of either $\alpha_{\tau(i)}\cdot\alpha_{\tau(j)}$ or $\alpha_{\tau(i)}(\alpha_{\tau(j)})^{-1}$ which is a simple closed curve. On S_α the primitive of either $\sigma_i+\sigma_j$ or $\sigma_i-\sigma_j$ induces a red-blue decomposition of S_α (see for example $\sigma_2+\sigma_4$ on $S_{\alpha_1\cdot\alpha_3}$ in *Figure 1*). Therefore we can proceed as in the previous subsection to obtain estimates on $\sigma_i+\sigma_j$ or $\sigma_i-\sigma_j$ on S_α and hence for q_{ij} using equation (6) and (7).
As it is in general difficult to find α, we will present this approach only in the case, where $\alpha_j=\alpha_{\tau(i)}$. We present these estimates in *Case 1.* If $\alpha_j\neq\alpha_{\tau(i)}$, we will present an alternative approach in *Case 2.* We will make use of both methods in section 4.2.

Case 1: Estimates for $q_{i\tau(i)}$

Consider WLOG q_{12}. Consider the simple closed geodesic α_{12} in the free homotopy class of $\alpha_{12}=\alpha_1\,{\alpha_2}^{-1}$. Due to the relationships in equation (8), $\sigma_1+\sigma_2$ has a primitive F_{12} on $S_{\alpha_{12}}=S_{12}$ that induces a red-blue decompositon of S_{12}. We embed S_{12} into a cylinder C. We also denote the embedded surface by S_{12}.
As in the previous subsection, the capacity $\text{cap}(S_{12})$ provides an upper bound for $E(\sigma_1+\sigma_2)$:

$$\text{cap}(S_{12})\geq E(\sigma_1+\sigma_2).$$

We obtain a lower bound for $E(F_{12})=E(\sigma_1+\sigma_2)$ from the red-blue decomposition induced by F_{12} on on S_{12}. Here we can use the same methods as for $E(\sigma_1)$ on S_2 presented in the previous subsection.
With the estimates for $E(\sigma_1+\sigma_2)$, $E(\sigma_1)$ and $E(\sigma_2)$ applied to equation (6), we obtain an upper and lower bound on q_{12}.

Case 2: Estimates for $q_{ij}, j\neq\tau(i)$

In this case α_i and α_j do not intersect. Consider WLOG q_{13}. For $\alpha_{\tau(1)}=\alpha_2$ and $\alpha_{\tau(3)}=\alpha_4$ consider $S_{\alpha_2\cup\alpha_4}=S_{24}$. S_{24} consists out of two connected parts. Let $S_{24}^1\subset S_{\alpha_2}$ be the part that contains α_2 and let $S_{24}^3\subset S_{\alpha_4}$ be the part that contains α_4. We embed S_{24}^1 into a cylinder C_1 around α_2 and S_{24}^3 into a cylinder C_3 around α_4 and denote the embedded surfaces by the same name. Due to the relationships in equation (8), $\sigma_1+\sigma_3$ has a primitive on both $S_{24}^1\subset C_1$ and $S_{24}^3\subset C_3$. Such a decomposition is shown in *Figure 2.*
For $i\in\{1,3\}$, let $\tilde{F}_i$ on S_{24}^i be a function that satisfies boundary conditions for the capacity problem on S_{24}^i. Then these functions together define naturally a function $\tilde{F}_{13}$ on S_{24}. By

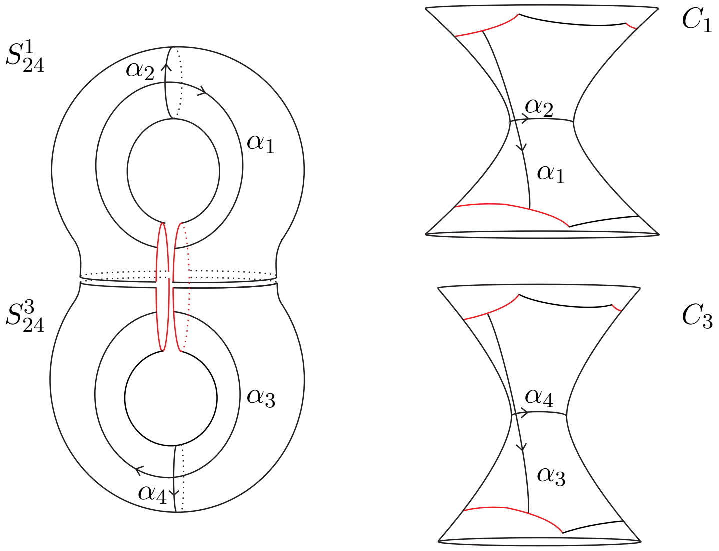

Figure 2: Embedding of S^i_{24} in a cylinder C_i around $\alpha_{\tau(i)}$ for $i \in \{1,3\}$.

smoothing $\tilde{F}_{13}$ in an inner environment of the boundary of S_{24}, we obtain a function $\tilde{f}_{13}$ on S, whose derivative $d\tilde{f}_{13}$ is a closed differential form that satisfies the same integral conditions on the cycles as $\sigma_1 + \sigma_3$. Due to the energy-minimizing property of $\sigma_1 + \sigma_3$ we have that $E(\tilde{f}_{13}) \geq E(\sigma_1 + \sigma_3)$. Hence the sum of the capacities of S^1_{24} and S^3_{24} provides an upper bound for $E(\sigma_1 + \sigma_3)$:

$$\mathrm{cap}(S^1_{24}) + \mathrm{cap}(S^3_{24}) \geq E(\sigma_1 + \sigma_3).$$

We obtain a lower bound for $E(\sigma_1 + \sigma_3)$ by applying the methods used to obtain a lower bound on $E(\sigma_1)$ on S_2 presented in the previous subsection. Here we obtain estimates from the red-blue decompostions induced by the primitive F_{13} of $\sigma_1 + \sigma_3$ on S^1_{24} in C_1 and S^3_{24} in C_3. The only difference is that we have some segments of the boundary, where the red-blue decomposition does not apply. Here we disregard these pieces in the construction of S^{1red}_{24} and S^{3red}_{24}. As these sets are disjoint we are looking for a certain function f_{13} that satisfies

$$f_{13}(p_2) - f_{13}(p_1) = F_{13}(p_2) - F_{13}(p_1) = 1$$

for all points p_1, p_2 in ∂S^{1red}_{24} or ∂S^{3red}_{24}. Let p_φ be the projection of a vector field in the tangent space onto lines of a suitable parametrization φ of S^{1red}_{24} and S^{3red}_{24}. Let f_{13} is the function that minimizes the projected energy $E(p_\varphi(D\cdot))$. We then obtain with $S^r_{24} = S^{1red}_{24} \cup S^{3red}_{24}$:

$$E(\sigma_1 + \sigma_3) \geq E_{S^r_{24}}(p_\varphi(Df_{13})).$$

With the estimates for $E(\sigma_1 + \sigma_3)$, $E(\sigma_1)$ and $E(\sigma_3)$ applied to equation (6), we obtain an upper and lower bound on q_{13}:

$$\begin{aligned} q_{13} &\geq \frac{1}{2}\left(E_{S^r_{24}}(p_\varphi(Df_{13})) - \mathrm{cap}(S_{\alpha_2}) - \mathrm{cap}(S_{\alpha_4})\right) < 0 \quad \text{and} \\ q_{13} &\leq \frac{1}{2}\left(\mathrm{cap}(S^1_{24}) + \mathrm{cap}(S^3_{24}) - E_{S^{red}_{\alpha_2}}(p_\varphi(Df_1)) - E_{S^{red}_{\alpha_4}}(p_\varphi(Df_3))\right) > 0. \end{aligned} \tag{10}$$

Here f_3 is the minimizing function corresponding to the primitve F_3 of σ_3 on $S_{\alpha_4}^{red}$ constructed analogously to f_1 in the previous subsection. Using this approach we can only obtain optimal estimates, if q_{13} is close to zero. This is due to the fact that we do not have full information of the boundary values on our tubes S_{24}^3 and S_{24}^1. This estimate is however better than the one obtained from equation (5). As was shown in [BMMS], the value of q_{13} is always close to zero, if α_2 and α_4 are separated by a small scg γ.

We now give two examples to demonstrate the weakness and strength of the method. We first show that the energy of a dual harmonic form can be lower than the capacity of a cylinder of even infinite length. The following example is due to Peter Buser.

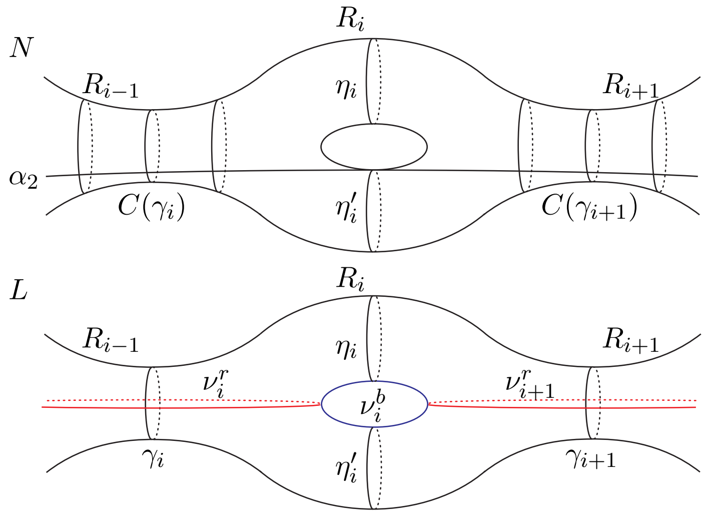

Figure 3: Building blocks for the surfaces N and L of genus g.

Example 1: For comparison we briefly review here the example of the necklace surface given in [BSe1]. Let Y be a Y-piece, a surface of signature $(0,3)$. Let γ, η and η' be its boundary geodesics, such that η and η' have equal length. We paste two copies of Y along η and η' to obtain R of signature $(1,2)$. The necklace surface N of genus g, is obtained by pasting together $g-1$ copies $R_1, ...R_{g-1}$ of a building block R as shown in *Figure 3*. Here the free boundary of R_{g-1} is pasted along γ_1 of R_1 to obtain a ring. By the collar lemma (see [Bu], p. 106), each γ_i has a collar of width w_γ, where

$$w_\gamma \geq \operatorname{arcsinh}\left(\frac{1}{\sinh(\frac{\gamma}{2})}\right).$$

Let A $= (\alpha_1, \alpha_{\tau(1)}, ..., \alpha_g, \alpha_{\tau(g)})$ be a canonical homology basis, such that $\alpha_1 = \gamma_1$ and $\alpha_{\tau(1)} = \alpha_2$ is a simple closed geodesic that intersects all γ_i exactly once. Let Q_S be the corresponding period Gram matrix. We will examine the upper bound on the entry $q_{22} = E(\sigma_2)$.

Following our method we have to embed $S_1 = S_{\alpha_1}$ into a cylinder C_1 and have to evaluate $\text{cap}(S_1)$. Now if an annulus A is contained in an annulus B then $\text{cap}(A) \geq \text{cap}(B)$. Therefore

$\mathrm{cap}(S_1) \geq \mathrm{cap}(C_1)$. The capacity of the cylinder C_1 with baseline of length $l(\alpha_1) = l(\gamma)$ of infinite width is not zero. This follows from equation (2). We have that

$$\mathrm{cap}(S_1) \geq \mathrm{cap}(C_1) = \frac{l(\gamma)}{\pi}.$$

We now give another estimate for the energy of σ_2 with the help of a test form s_2. This approach applies only to this example. To this end consider the collar $C(\gamma_i)$ of a γ_i. On each $C(\gamma_i)$ set $s_2 = dF_2$, where dF_2 is the real harmonic function that has value 0 on one boundary of $C(\gamma_i)$ and $\frac{1}{g-1}$ on the other. We set $s_2 = 0$ on $S \backslash \bigcup_{i=1}^{g-1} C(\gamma_i)$. Then s_2 is arbitrarily close to a closed form that satisfies the same conditions on the cycles of A as σ_2 and we have

$$E(\sigma_2) < E(s_2) \leq (g-1) \cdot \frac{(g-1)^{-2} \cdot l(\gamma)}{\pi - 2\arcsin\left(\frac{1}{\cosh(w_\gamma)}\right)},$$

where w_γ is bounded from below by the collar lemma. Hence $E(\sigma_2)$ is at most of order $\frac{1}{g}$ and goes to zero, as g goes to infinity. Our upper bound, on the contrary, is always bigger than the constant $\frac{l(\gamma)}{\pi}$. This shows that there exist examples where our upper bound can not be of the right order. This might be due to the fact that the projection of $CL^{blue}(\alpha_1)$ onto α_1 can attain almost the length of α_1. Hence as S_1^{blue} is large, $E(\sigma_2)$, the energy of σ_2 might be small. However it might be possible to obtain a better result by adjusting the boundary values on $CL^{blue}(\alpha_1)$ as described in the discussion of the upper bound.

Example 2: For our second example we construct a linear surface L of genus g. This example belongs to the class of M-curves described in [BSi]. In this construction we use Y-pieces Y, where the length of η and η' is large. We construct R from two copies of these Y-pieces as in the previous example. To construct a surface L of genus g, we paste together $g-2$ copies $R_2, ...R_{g-1}$ along the γ_i. Then we paste two copies of Y, Y_1 and Y_g on each side of R_2 and R_{g-1}, respectively. We close these Y pieces by pasting them together along η and η'. We call the image of η in Y_i η_i for $i \in \{1, g\}$ (see *Figure 3*).
Let A $= (\alpha_1, \alpha_{\tau(1)}, ..., \alpha_g, \alpha_{\tau(g)})$ be a canonical homology basis, such that $\alpha_1 = \eta_1$ and $\alpha_{\tau(1)} = \alpha_2$ the unique simple closed geodesic in Y_1 that intersects α_1 perpendicularly. Let Q_S be the corresponding period matrix. We now show that in this case, the upper bound for $q_{22} = E(\sigma_2)$ is optimal. Therefore we use the symmetries of the surface L.
It is easy to see that $CL(\alpha_1)$, the cut locus of α_1 in L consists of the scgs ν_i^r that intersect the geodesics γ_i perpendicularly and the scgs $\nu_i^b \subset R_i$ that intersect the scgs η_i and η_i' perpendicularly (see *Figure 3*). We have:

$$CL(\alpha_1)^{red} = \{\nu_1^r, ..., \nu_g^r\} \quad \text{and} \quad CL(\alpha_1)^{blue} = \{\nu_2^b, ..., \nu_{g-1}^b\} \cup \eta_g.$$

We now consider the following two isometries ϕ_1 and ϕ_2 in $\mathrm{Isom}(L)$. ϕ_1 is the hyperelliptic involution that fixes the cut locus $CL(\alpha_1)$ as a set, such that $\phi_1(\eta_i) = \eta_i'$ for all i. ϕ_2 is the isometry that fixes $CL(\alpha_1)$ as a set and all ν_i^b point-wise. Set $\phi = \phi_1 \circ \phi_2$. ϕ is the isometry that maps any point p in $CL(\alpha_1)^{red} \subset S_1$ to the corresponding point p' in the red-blue composition induced by σ_2.
Consider now the primitive F_2 of σ_2 on $S_{\alpha_1} = S_1$. We have that $F_2 \circ \phi_2$ is a harmonic function,

whose derivative $d(F_2 \circ \phi_2)$ defines a 1-form σ_2' on S. σ_2' satisfies the same conditions on the cycles as σ_2. Due to the uniqueness of σ_2 we have $\sigma_2' = \sigma_2$ and we have $F_2 \circ \phi_2 = F_2$. In the same way $1 - F_2 \circ \phi_1$ is a harmonic form, whose derivative $-d(F_2 \circ \phi_1)$ defines a 1-form σ_2'' on S that satisfies the same integral conditions on the cycles as σ_2. Hence we have $\sigma_2'' = \sigma_2$. By choosing an appropriate additive constant, we obtain:

$$F_2 \circ \phi_2 = F_2 \quad \text{and} \quad 1 - F_2 \circ \phi_1 = F_2.$$

Now for any p on one side of $CL(\alpha_1)^{red} \subset S_1$ we have that $F_2(p) - F_2(\phi(p)) = 1$. Together with the above equation we obtain:

$$F_2(\phi(p)) = 0 \quad \text{and} \quad F_2(p) = 1.$$

Hence the red parts of the boundary satisfy the conditions for the capacity problem. Now for large η, we have from hyperbolic geometry that $l(\nu_i^b)$ is arbitrarily small. Hence in this case we obtain

$$q_{22} = E(\sigma_2) = \text{cap}(S_1) - \epsilon$$

and our upper bound for a diagonal entry of Q_S is sharp.

4 Estimates for the period Gram matrix based on Q-pieces

In this section we establish upper and lower bounds for all entries of the period Gram matrix based on the geometry of the Q-pieces. All formulas concerning the geometry of hyperbolic polygons in this section can be found in [Bu], p. 454.

Let S is a Riemann surface of genus $g > 2$ and A a canonical homology basis. Then the pairs $((\alpha_i, \alpha_{\tau(i)}))_{i=1,3,..2g-1}$ are contained in disjoint surfaces of signature $(1,1)$ or Q-pieces. If $g = 2$, then the Q-pieces intersect at the boundary, but this will not concern us here. Let $(Q_i)_{i=1,3,..,2g-1}$ be a set of Q-pieces, such that

$$(\alpha_i, \alpha_{\tau(i)}) \subset Q_i = Q_{\tau(i)} \quad \text{for} \quad i \in \{1, 3, .., 2g-1\}.$$

We will present estimates on the entries of the period Gram matrix Q_S using a partition of S that contains these pieces. To establish these estimates, the following information about the geometry of the Q-pieces $(Q_i)_{i=1,3,..,2g-1}$ must be known.

Let β_i be the boundary geodesic of Q_i and let $\alpha_{i\tau(i)} \subset Q_i$ be the simple closed geodesic in the free homotopy class of $\alpha_i(\alpha_{\tau(i)})^{-1}$. If we cut open Q_i along one of these three geodesics, Q_i decomposes into a Y-piece. Let $t_j \in]-\frac{1}{2}, \frac{1}{2}]$ be the twist parameter (see [Bu], p. 29) for the decomposition with α_j, where $j \in \{i, \tau(i), i\tau(i)\}$. To obtain practical estimates on all entries of the matrix Q_S, we assume that the following parameters are known for each Q_i:

- the length of β_i
- the length of $\alpha_i, \alpha_{\tau(i)}$ and $\alpha_{i,\tau(i)}$
- the twist parameters t_j for $j \in \{i, \tau(i), i\tau(i)\}$

A Q-piece Q_i is already determined by a triplett (β_i, α_k, t_k), where $k \in \{i, \tau(i), i\tau(i)\}$ and these Fenchel-Nielsen coordinates are a common way to provide the data for a Q-piece. Therefore we will first show how to obtain the remaining information in the list above from such a description.

Then we will give a parametrization of trirectangles. The formulas developed here, will be used in the final subsection. All formulas in this section have been implemented in a MAPLE sheet, so that concrete estimates can be obtained from the above input.

Let WLOG $Q_i = Q_1$. We assume that Q_1 is given in the Fenchel-Nielsen coordinates (β_1, α_1, t_1).

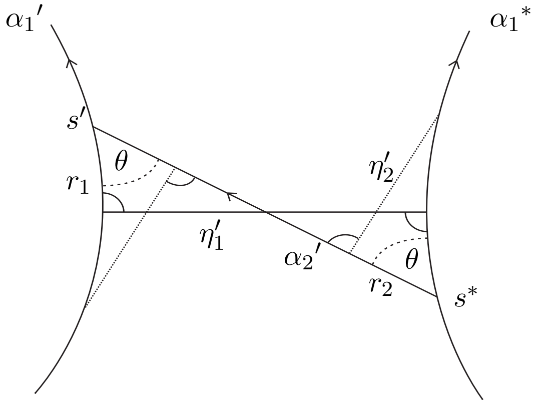

Figure 4: Two lifts of α_1 in the universal covering

We assume furthermore that

$$\cosh(\frac{\alpha_1}{2}) \leq \cosh(\frac{\beta}{6}) + \frac{1}{2}. \tag{11}$$

Such a short α_1 exists indeed. This is stated in [Pa], **Proposition 5.4**. This assumption simplifies the calculation of the twist parameters t_2 and t_{12}. As we will see in the following this choice of a small α_1 also improves our estimates.

In Q_1 there exists a unique shortest geodesic arc η_1 meeting α_1 perpendicularly on both sides of α_1. *Figure 4* shows a lift of α_1 and η_1 in the universal covering. Here α_1 lifts to ${\alpha_1}'$ and ${\alpha_1}^*$ and η_1 to η_1'. Note that ${\alpha_1}'$ and ${\alpha_1}^*$ have the same orientations with respect to η_1'. In the covering there exist two points, $s' \in {\alpha_1}'$ and $s^* \in {\alpha_1}^*$, on opposite sites of η_1' and at the same distance from η_1', such that s' and s^* are mapped to the same point $s \in \alpha_2$ by the covering map. Observe that we can always find s' and s^*, such that the distance r_1 from η_1' is equal to $\frac{\alpha_1 \cdot t_1}{2}$. We denote by ${\alpha_2}'$ the the geodesic from s' to s^*. From ${\alpha_2}'$ we obtain two isometric right-angled geodesic triangles. Since ${\alpha_2}'$ intersects s' and s^* under the same angle θ, the image α_2 of ${\alpha_2}'$ under the universal covering map is a smooth simple closed geodesic, which intersects α_1 exactly once. Hence we can incorporate α_2 into our homology basis for S. Applying the cosine formula to one of the isometric triangles, we obtain:

$$\cosh(\frac{\alpha_2}{2}) = \cosh(r_1)\cosh(\frac{\eta_1}{2}), \quad \text{where} \quad r_1 = \frac{\alpha_1 \cdot t_1}{2}.$$

Here the length of η_1 can be calculated from a decomposition of Q_1 into a Y-piece (see equation (14). We have:

$$\sinh(\frac{\eta_1}{2}) = \frac{\cosh(\frac{\beta_1}{4})}{\sinh(\frac{\alpha_1}{2})} \Leftrightarrow \cosh(\frac{\eta_1}{2}) = \sqrt{\left(\frac{\cosh(\frac{\beta_1}{4})}{\sinh(\frac{\alpha_1}{2})}\right)^2 + 1}.$$

For further calculations we also need the angle θ. From hyperbolic geometry we obtain:

$$\cos(\theta) = \tanh(\frac{\alpha_1 \cdot t_1}{2})\coth(\frac{\alpha_2}{2}) \tag{12}$$

In Q_1 there exists likewise a unique shortest geodesic arc η_2 meeting α_2 perpendicularly on both sides of α_2. This arc can be seen in *Figure 4*. Now α_2 and α_1 intersect exactly once under the angle θ. Consider the right-angled triangle with sides $\frac{\alpha_1}{2}, r_2$ and $\frac{\eta_2}{2}$. Here r_2 contains information about the twist parameter t_2 with respect to α_2. We have:

$$\cos(\theta) = \tanh(r_2)\coth(\frac{\alpha_1}{2}).$$

Together with equation (12), we obtain:

$$\tanh(r_2) = \frac{\tanh(\frac{\alpha_1 \cdot t_1}{2})\coth(\frac{\alpha_2}{2})}{\coth(\frac{\alpha_1}{2})} \quad \text{and} \quad t_2 = \min(\frac{2r_2}{\alpha_2}, 1 - \frac{2r_2}{\alpha_2}).$$

We will now look for a suitable α_{12}. Consider again the lifts of α_1 in *Figure 4*. Consider the two points, $S' \in {\alpha_1}'$ and $S^* \in {\alpha_1}^*$ on the opposite side of s' and s^* with respect to the intersection point with η_1 and with distance $\alpha_1 - r_1$ from η_1'. S' and S^* are mapped to the same point $S \in Q$ by the covering map. Connecting these points we obtain a geodesic arc α_{12}', which maps to a scg α_{12} in Q. It follows from the intersection properties with α_1 and α_2 that α_{12} is in the free homotopy class $\alpha_1(\alpha_2)^{-1}$. Using the same reasoning as for α_2, we can find it's length and the twist parameter t_{12}.

4.1 Upper bounds based on trirectangles

Let C be a hyperbolic cylinder with baseline γ. Let $T \subset C$ be a hyperbolic trirectangle, which has one side d on $\gamma \subset C$ and such that the two adjacent sides meet d perpendicularly. A lift of C together with T into the universal covering is shown in *Figure 5*.

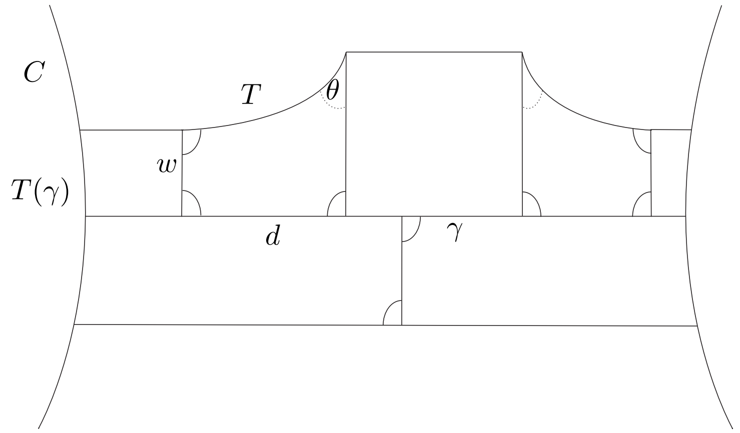

Figure 5: A lift of a cylinder C with baseline γ with a tube $T(\gamma)$ containing the trirectangle T in the universal covering.

We assume that T is given in Fermi coordinates by

$$T = \psi(\{(t,s) \mid s \in [0, a_2(t)], t \in [0,d]\}),$$

where, by abuse of notation, d denotes the length of d. We assume furthermore that the shortest side of T, which is perpendicular to d has length w and intersects d in $\psi(0,0)$. For $t \in [0,d]$, we have

$$a_2(t) = \operatorname{arctanh}\left(\frac{\cosh(t)}{\coth(w)}\right), \quad \text{where} \quad d < \operatorname{arcsinh}\left(\frac{1}{\sinh(w)}\right). \tag{13}$$

This follows from the geometry of trirectangles. With **Theorem 3.1**, we obtain the following lemma:

Lemma 4.1 *Let C be a hypberbolic cylinder with baseline γ. Let $T(\gamma) \subset C$ be a topological tube around γ, whose boundary segments consist of either boundary arcs of trirectangles or curves contained in a distance set $\partial Z_r(\gamma)$ for some r. Then we have for $H(s) = 2\arctan(\exp(s))$ and $q_i(t) = \frac{\partial H(s_0)}{\partial s}|_{s_0 = a_i(t)} \cdot a_i'(t)$:*

$$\int_0^{l(\gamma)} \frac{1 + \frac{q_1(t)^2 + q_1(t)q_2(t) + q_2(t)^2}{3}}{H(a_2(t)) - H(a_1(t))}\, dt \geq \operatorname{cap}(T(\gamma)) \geq \int_0^{l(\gamma)} \frac{1}{H(a_2(t)) - H(a_1(t))}\, dt$$

If a boundary segment $\partial T = \psi(\{(t,s) \mid t \in [0,d], s = a_2(t), 0 < w = a_2(0) < a_2(d)\}) \subset \partial T(\gamma)$ belongs to a trirectangle T then

$$H(a_2(t)) = 2\arctan\left(\sqrt{\frac{\coth(w) + \cosh(t)}{\coth(w) - \cosh(t)}}\right) \quad \text{and} \quad q_2(t) = \frac{\sinh(t)}{\sqrt{\coth(w)^2 - \cosh(t)^2}}.$$

Such a tube $T(\gamma)$ is depicted in *Figure 5*. This lemma follows directly from equation (13), the formulas for $H(s)$ and $q_i(t)$ and the fact that $\frac{1}{\cosh(\operatorname{arctanh}(x))} = \sqrt{1 - x^2}$ and $\exp(\operatorname{arctanh}(x)) = \sqrt{\frac{1+x}{1-x}}$. A parametrisation of other boundary parts of $T(\gamma)$ can be easily obtained by adapting the above formulas.

The relation with our problem of providing estimates for the energy of dual harmonic forms is the following. Let S be a Riemann surface and A a canonical homology basis. If $\gamma = \alpha_{\tau(i)}$ for some $\alpha_{\tau(i)} \in$ A and $T(\alpha_{\tau(i)})$ is contained in $S_{\alpha_{\tau(i)}} \subset C$, then the capacity of $T(\alpha_{\tau(i)})$ provides an upper bound for the entry q_{ii} of the period Gram matrix Q_S.

$$\operatorname{cap}(T(\alpha_{\tau(i)})) > q_{ii}.$$

We will make use of these formulas in the following section.

4.2 Upper bounds for the entries of Q_S based on the geometry of Q-pieces

We will establish estimates for all entries of the period Gram matrix based on the geometry of the Q-pieces $(Q_i)_{i=1,3,..,2g-1}$. Following the approach given in section 3.1, it is sufficient to construct suitable functions on

$$S_\gamma \cap Q_i, \quad \text{where} \quad \gamma \in \{\alpha_i, \alpha_{\tau(i)}, \alpha_{i\tau(i)}\}, \quad \text{for} \quad i \in \{1,3,..,2g-1\}.$$

In this section we will only show how to obtain estimates for q_{11} based on the geometry of Q_1. These estimates will only depend on the Fenchel-Nielsen coordinates (β_1, α_2, t_2) of Q_1. In the same way we obtain estimates for q_{22} and q_{12} based on the coordinates, (β_1, α_1, t_1) and $(\beta_1, a_{12}, t_{12})$ of Q_1. Proceeding the same way on the remaining Q-pieces and combining these

estimates as described in section 3.2 we finally obtain estimates for all entries of the period matrix.
To obtain an upper bound for q_{11} we embed $S_{\alpha_2} \cap Q_1$ into a hyperbolic cylinder C with baseline α_2 and denote this embedding by the same name. To obtain an estimate on q_{11} we will give a parametrization of

$$S_{\alpha_2} \cap Q_1 \subset C$$

based on a decomposition into trirectangles. We will give a description of $S_{\alpha_2} \cap Q_1$ that depends only on the length of α_2, $\beta = \beta_1$ and the twist parameter t_2.

To obtain this parametrization, we first cut open Q_1 along α_2 to obtain the Y-piece Y_1 with boundary geodesics β, ${\alpha_2}'$ and ${\alpha_2}''$. ${\alpha_2}'$ and ${\alpha_2}''$ have length α_2 (see *Figure 6*). Denote by b the shortest geodesic arc connecting ${\alpha_2}'$ and ${\alpha_2}''$. Now we cut open Y_1 along the shortest geodesic arcs connecting β and the other two boundary geodesics. We call Y_1' the surface, which we obtain by cutting open Y_1 along these lines. By abuse of notation, we denote the geodesic arcs in Y_1' by the same letter as in Y_1. The geodesic arc b divides Y_1' into two isometric hexagons H_1 and H_2. This decomposition is also shown in *Figure 6*.

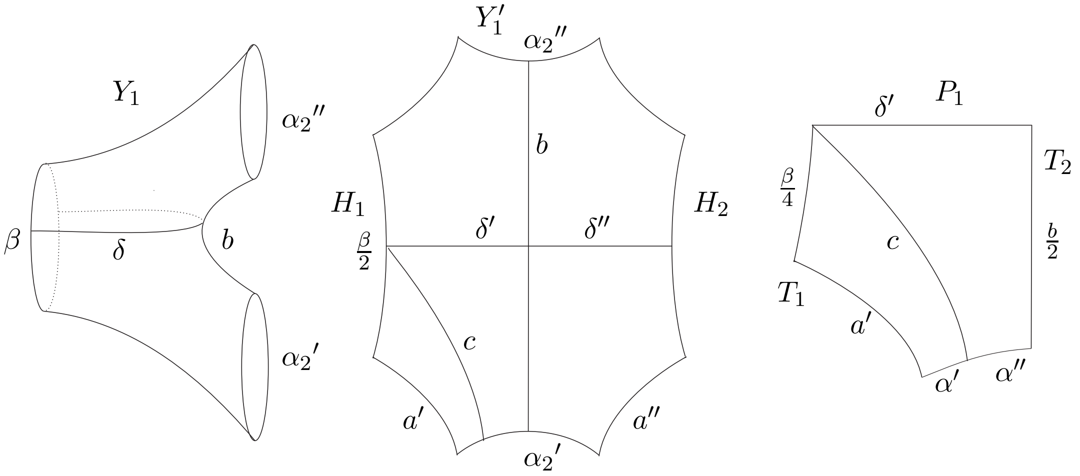

Figure 6: Decomposition of Y_1 into isometric hexagons H_1 and H_2.

In H_1 b is the boundary geodesic connecting $\frac{{\alpha_2}'}{2}$ and $\frac{{\alpha_2}''}{2}$. Denote by δ' the shortest geodesic arc in H_1 connecting b and the side opposite of b of length $\frac{\beta}{2}$. By abuse of notation we denote this side by $\frac{\beta}{2}$. We denote by δ'' the arc in H_2 corresponding to δ' in H_1. Let δ be the geodesic arc in Y_1', such that $\delta = \delta' \cup \delta''$. It is easy to see that the geodesic arc in Q_1 that maps to δ in Y_1' constitutes the intersection of the cut locus of α_2 with Q_1. We denote this geodesic arc in Q_1 and Y_1 also by δ:

$$\delta = CL(\alpha_2) \cap Q_1.$$

We denote furthermore by a' the geodesic arcs connecting $\frac{{\alpha_2}'}{2}$ and $\frac{\beta}{2}$ in H_1 and by a'' the corresponding arc in H_2. Let a be the length of such an arc.
δ' divides H_1 into two isometric right-angled pentagons P_1 and P_2. Let P_1 be the pentagon that has $\frac{{\alpha_2}'}{2}$ as a boundary. To establish the parametrization for $S_{\alpha_2} \cap Q_1$, we divide P_1 into two

trirectangles.
Let c be the geodesic arc in P_1 that emanates from the vertex, where $\frac{\beta}{2}$ and δ intersect and that meets $\frac{\alpha_2{}'}{2}$ perpendicularly. It divides $\frac{\alpha_2{}'}{2}$ into two parts, α' and α'' (see *Figure 6*). c divides P_1 into two trirectangles, T_1, which has the boundary α' and T_2, which has the boundary α''.
To obtain an upper bound for q_{11}, we have to know the geometry of T_1 and T_2. To apply the results from the previous subsection, we have to know the lengths a, α', α'' and $\frac{b}{2}$.
In the following subsection we will also need the length of c, which we will calculate here. To obtain these lengths, we will use the geometry of H_1, P_1, T_1 and T_2.

From the geometry of the hyperbolic pentagon P_1 we have:

$$\begin{aligned}\cosh(\frac{\beta}{4}) &= \sinh(\frac{\alpha_2}{2})\sinh(\frac{b}{2}) \Leftrightarrow \sinh(\frac{b}{2}) = \frac{\cosh(\frac{\beta}{4})}{\sinh(\frac{\alpha_2}{2})} && (14)\\ \cosh(\delta') &= \sinh(\frac{\alpha_2}{2})\sinh(a). && (15)\end{aligned}$$

Hence we obtain b from equation (14).

From the geometry of the hyperbolic hexagon H_1 and as $\sinh(b) = 2\sinh(\frac{b}{2})\cosh(\frac{b}{2})$ and $\cosh(b) = 2\cosh(\frac{b}{2})^2 - 1$, we obtain now a:

$$\coth(a) = \frac{\sinh(b)\cosh(\frac{\alpha_2}{2})}{1+\cosh(b)} = \tanh(\frac{b}{2})\cosh(\frac{\alpha_2}{2}). \tag{16}$$

From equation (15) and (16) and as $\sinh(\operatorname{arccoth}(x)) = \frac{1}{\sqrt{x^2-1}}$ we obtain $\delta' = \frac{\delta}{2}$:

$$\cosh(\delta') = \frac{\sinh(\frac{\alpha_2}{2})}{\sqrt{\tanh(\frac{b}{2})^2\cosh(\frac{\alpha_2}{2})^2 - 1}}. \tag{17}$$

Finally from the geometry of hyperbolic trirectangles T_1 and T_2 we obtain :

$$\begin{aligned}\coth(\alpha'') &= \frac{\cosh(\frac{b}{2})}{\tanh(\delta')}. && (18)\\ \sinh(c) &= \cosh(\delta')\sinh(\frac{b}{2}). && (19)\end{aligned}$$

As $\alpha' = \frac{\alpha_2}{2} - \alpha''$, it remains to express α'' in terms of α_2 and b. From equation (17) and (18) we obtain with $\frac{1}{\tanh(\operatorname{arccosh}(x))} = \frac{x}{\sqrt{x^2-1}}$ that

$$\coth(\alpha'') = \frac{\cosh(\frac{b}{2})^2\sinh(\frac{\alpha_2}{2})}{\sqrt{\cosh(\frac{b}{2})^2\sinh(\frac{\alpha_2}{2})^2 - (\sinh(\frac{b}{2})^2\cosh(\frac{\alpha_2}{2})^2 - \cosh(\frac{b}{2})^2)}}.$$

As $\sinh(x)^2 = \cosh(x)^2 - 1$, this simplifies to

$$\coth(\alpha'') = \cosh(\frac{b}{2})^2\tanh(\frac{\alpha_2}{2}). \tag{20}$$

Finally we obtain for c from equation (14), (17) and (19) and as $\sinh(x)^2 = \cosh(x)^2 - 1$:

$$\sinh(c) = \frac{\cosh(\frac{\beta}{4})}{\sqrt{\tanh(\frac{b}{2})^2 \cosh(\frac{\alpha_2}{2})^2 - 1}}. \tag{21}$$

Hence can express the length of b, a, α'' and $\alpha' = \frac{\alpha_2}{2} - \alpha''$ in terms of α_2 and β - see equation (14), (16) and (20), respectively.

With these formulas we are now able to obtain a description of the boundary of $S_{\alpha_2} \cap Q_1 \subset C$. Consider now $\delta \subset Y_1'$. δ divides Y_1' into two isometric hexagons. Let H_1' be the hexagon that contains ${\alpha_2}'$ as a boundary geodesic and H_2' be the hexagon that contains ${\alpha_2}''$ as a boundary geodesic δ forms the cut locus of α_2 in Q_1. Denote by Q_1' the surface that we obtain if we cut open Q_1 along δ. Q_1' is a topological cylinder around α_2. A lift of Q_1' in the universal covering is depicted in *Figure 7*.

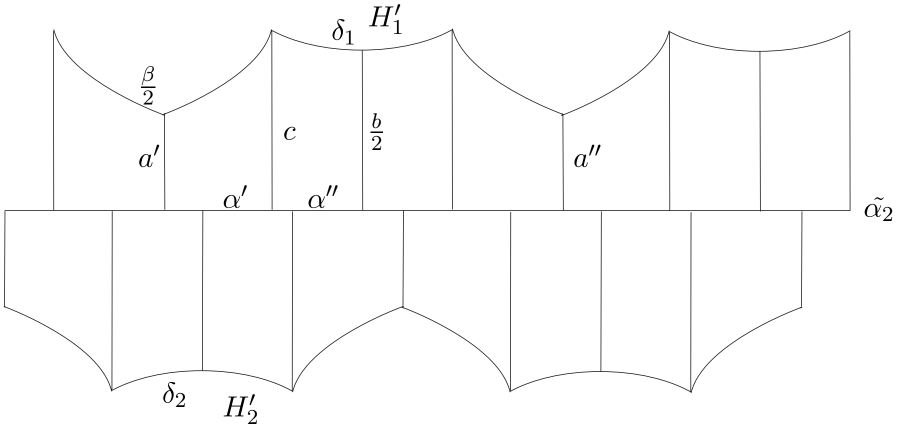

Figure 7: Lift of Q_1' into the universal covering.

By abuse of notation we denote by H_1' and H_2' two hexagons in this lift, which are isometric to the hexagons with the same name in Y_1' and that are adjacent along the lift $\tilde{\alpha_2}$ of α_2. We keep the notation from Y_1', but denote by $\delta_i \subset H_i'$, for $i \in \{1, 2\}$, the two sides corresponding to δ in Y_1'. In the lift of Q_1' the two hexagons H_1' and H_2' are shifted against each other by the length $t_2 \cdot \alpha_2$. It is easy to see from *Figure 7*, how to parametrize $S_{\alpha_2} \cap Q_1$ in a cylinder C around α_2. Here all boundaries are boundaries of trirectangles, which are isometric to either T_1 or T_2. Hence $S_{\alpha_2} \cap Q_1 = T(\alpha_2)$ satisfies the conditions of **Lemma 4.1**. Adapting the formulas given in this lemma, we can find an upper bound for

$$\operatorname{cap}(S_{\alpha_2} \cap Q_1) \geq q_{11}.$$

Remark: From numerical simulations we get the following impression. If the length of α' or α'' is near the maximal possible value $\operatorname{arcsinh}(\frac{1}{\sinh(a)})$ or $\operatorname{arcsinh}(\frac{1}{\sinh(\frac{b}{2})})$, respectively, then our test function is not well suited for the capacity problem and overestimates the capacity of $S_{\alpha_2} \cap Q_1$ and therefore also $E(\sigma_1)$. Here we can improve our estimate by cutting of these pointy edges at the endpoints of δ_1 and by replacing them with a suitable boundary of constant distance from

α_2 (see *Figure 5*).
We also obtain an upper bound for $E(\sigma_1)$ from the capacity $\text{cap}(C(\alpha_2))$ of a collar around α_2 (see equation (2)). The upper bound from $\text{cap}(S_{\alpha_2} \cap Q_1)$ seems to be improving the estimate from $\text{cap}(C(\alpha_2))$ if $\min\{a, \frac{b}{2}\}$ is small. For $\min\{a, \frac{b}{2}\} > 4$ hardly any improvement can be obtained.

4.3 Lower bounds on the entries of Q_S based on Q-pieces

Consider the primitive F_1 of σ_1 in $Q'_1 = S_{\alpha_2} \cap Q_1 \subset C$. The two geodesic arcs δ_1 and δ_2 corresponding to $\delta \subset Q_1$ constitute $CL(\alpha_2)^{red} \cap \partial Q'_1$. We will use the theoretical approach from section 3 to obtain a concrete lower bound for

$$q_{11} = E_S(F_1) > E_B(F_1), \quad \text{where} \quad B = B_2 = S_2^{red} \cap Q'_1.$$

We will give a suitable construction for $B = S_2^{red} \cap Q'_1$ in the following. To this end we lift Q'_1 into the universal covering as in the previous subsection (see *Figure 7*). We use the same notation for the geodesic arcs that occur. The important cutout from *Figure 7* is depicted in *Figure 8*.

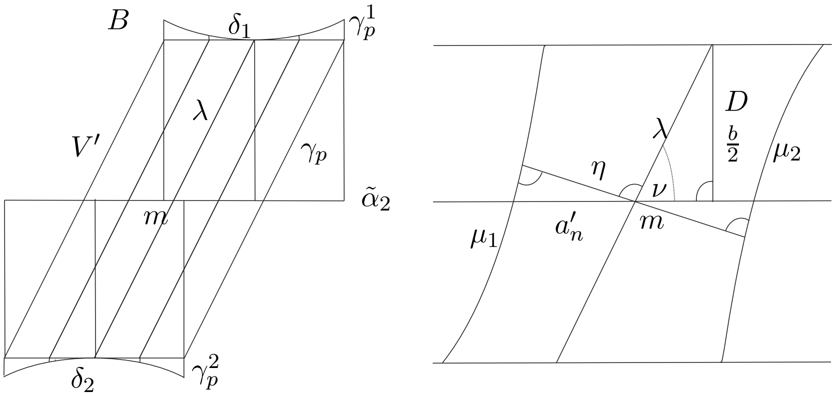

Figure 8: The area B and the construction of skewed Fermi coordinates ψ^ν.

Let B be the hatched subset in the lift of Q'_1 in *Figure 8*. We will give an exact description and parametrization of B in the following.
The boundary of B contains the lines δ_1 and δ_2. For each point $p_1 \in \delta_1$ there exists a point $p_2 \in \delta_2$, such that p_1 and p_2 map to the same point p on $\delta \subset Q_1$. We may assume WLOG that

$$F_1(p_2) - F_1(p_1) = 1 \quad \text{for all} \quad p_1 \in \delta_1$$

We will describe B as a set of lines, where each line l_p connects p_1 and p_2. l_p can be described in the following way. From p_1 we go along the geodesic that meets $\tilde{\alpha}_2$ perpendicularly until we meet $\partial Z_{\frac{b}{2}}(\tilde{\alpha}_2)$. We call this intersection point p'_1 and the geodesic arc that forms γ_p^1. Let p'_2 be the point on $\partial Z_{\frac{b}{2}}(\tilde{\alpha}_2)$ on the other side of $\tilde{\alpha_2}$ that can be reached analogously, starting from p_2. We now go along the geodesic arc that connects p'_1 and p'_2. We call this arc γ_p. Then from p'_2, we move along the geodesic arc connecting p_2' and p_2. We call this arc γ_p^2. We define l_p as the line traversed in this way. Let B be the disjoint union of these lines:

$$B = \biguplus_{p\in\delta} \{l_p\}$$

We will use a bijective parametrization φ of B. We want a $\varphi : (t,s) \mapsto \varphi(t,s)$ such that for a fixed $t_0 \in [-\alpha'', \alpha'']$, $\varphi(t_0, \cdot)$ parametrizes the line l_p that traverses $\tilde{\alpha_2}$ in a point with directed distance t_0 from m. We parametrize the sets $\bigcup\limits_{p\in\delta}\{\gamma_p^1\}$ and $\bigcup\limits_{p\in\delta}\{\gamma_p^2\}$ in Fermi coordinates with baseline $\tilde{\alpha_2}$. The proper parametrization can be deduced from the geometry of the trirectangle T_2.

We will parametrize $Z_{\frac{b}{2}}(\tilde{\alpha}_2) \cap B = \bigcup\limits_{p\in\delta}\{\gamma_p\}$ using *skewed Fermi coordinates* ψ^ν with angle ν and baseline $\tilde{\alpha_2}$. These are defined in the same way as the usual Fermi coordinates ψ (see section 1), but instead of moving along geodesics emanating perpendicularly from the baseline, we move along geodesics that meet the baseline under the angle ν. We will not give these coordinates explicitly, but will derive the essential information from the usual Fermi coordinates ψ.
Therefore let λ be the geodesic arc connecting the midpoints of δ_1 and δ_2. The midpoint m of λ and the endpoints of $\frac{b}{2}$ are the vertices of a right-angled triangle D (see *Figure 8*). In our case the angle ν for the coordinates ψ^ν is the angle of D at the midpoint m. It follows from the geometry of right-angled triangles that

$$\cosh(\frac{\lambda}{2}) = \cosh(\frac{b}{2})\cosh(\frac{\alpha_2\, t_2}{2}), \tag{22}$$

where we assume WLOG that the twist parameter t_2 is in the interval $[0, \frac{1}{2}]$. Otherwise the situation is symmetric to the depicted one. We have:

$$\sinh(\frac{\lambda}{2}) = \frac{\sinh(\frac{b}{2})}{\sin(\nu)}.$$

The equations for D imply with $\sinh(x)^2 = \cosh(x)^2 - 1$:

$$\sin(\nu) = \frac{\sinh(\frac{b}{2})}{\sqrt{\cosh(\frac{b}{2})^2\cosh(\frac{\alpha_2 t_2}{2})^2 - 1}}. \tag{23}$$

Consider the following geodesic arcs in $Z_{\frac{b}{2}}(\tilde{\alpha}_2) \cap B$. For a $n \in \mathbb{N}$ let a_n' be a geodesic arc of length $\frac{2\alpha''}{n}$ on $\tilde{\alpha}_2$ with midpoint m. λ intersects a_n' in m under the angle ν. This is depicted in *Figure 8*.
Let η' be a geodesic intersecting λ perpendicularly in m. Let furthermore μ_1 and μ_2 be two geodesic arcs with endpoints on $Z_{\frac{b}{2}}(\tilde{\alpha}_2)$ that intersect η' perpendicularly, such that each of the arcs passes through an endpoint of a_n' on each side of λ. Let furthermore η be the geodesic arc on η' with endpoints on μ_1 and μ_2. For fixed $n \in \mathbb{N}$, we denote by η_n the length of η and by μ^n the length of μ_1 and μ_2:

$$\eta_n = l(\eta) \quad \text{and} \quad \mu^n = l(\mu_1) = l(\mu_2).$$

By choosing usual Fermi coordinates with baseline η, we can parametrize the strip, whose boundary lines are μ_1 and μ_2 and two segments of $\partial Z_{\frac{b}{2}}(\tilde{\alpha}_2)$ (see *Figure 8*).
n such strips can be aligned next to each other to obtain a parametrization of $Z_{\frac{b}{2}}(\tilde{\alpha}_2) \cap B$. For $n \to \infty$ we obtain a parametrization ψ^ν of $Z_{\frac{b}{2}}(\tilde{\alpha}_2) \cap B$. We have:

$$\lim_{n\to\infty} n \cdot \eta_n = \sin(\nu) 2\alpha'' \quad \text{and} \quad \lim_{n\to\infty} \mu^n = \lambda.$$

Combining the parametrizations for the several pieces of B, we may assume that we have a parametrization φ that satisfies our conditions. For practical purposes, we extend the parametrization φ to the geodesics meeting $\partial Z_{\frac{b}{2}} \cap B$ perpendicularly in the direction opposite of $\tilde{\alpha_2}$.
Consider a point $p_1 = \varphi(t_0, -x) \in \delta_1$ and $p_2 = \varphi(t_0, x) \in \delta_2$. The function F_1 satisfies the boundary conditions $F_1(p_2) = 1 + \tilde{c}$ and $F_1(p_2) = \tilde{c}$, where $\tilde{c}$ is a constant. As we will see in the following, the constant $\tilde{c}$ is not important for our estimate and we assume that $\tilde{c} = 0$.
We consider the strip V, where

$$V = \varphi([t_0 - \epsilon, t_0] \times [-x, x]), \quad \text{where } \ \epsilon > 0 \text{ if } t_0 < 0 \text{ and } \epsilon < 0 \text{ if } t_0 > 0.$$

We will show, how to obtain a lower bound for the energy of $F_1|_V$, $E_V(F_1)$ for sufficiently small ϵ. We can align these strips to obtain a lower bound for $E_B(F_1) \leq E(F_1)$. We derive a lower bound for the energy of $F_1|_V$, assuming that

$$\begin{aligned} F_1|_{\varphi([t_0-\epsilon,t_0]\times\{-x\})} &= F_1(p_1) = 0 \quad \text{and} \quad F_1|_{\varphi([t_0-\epsilon,t_0]\times\{x\})} = F_1(p_2) = 1 \quad \text{and} \\ F_1|_{\varphi([t_0-\epsilon,t_0]\times\{\frac{-\lambda}{2}\})} &= F_1(p_1') = a_1' \quad \text{and} \quad F_1|_{\varphi([t_0-\epsilon,t_0]\times\{\frac{\lambda}{2}\})} = F_1(p_2') = a_2'. \end{aligned}$$

Consider the subset V' of V given by

$$V' = \varphi([t_0 - \epsilon, t_0] \times [\frac{-\lambda}{2}, \frac{\lambda}{2}]).$$

Let $F_{t_0} = f_{t_0} \circ \psi^\nu$ be a function defined on V' that realizes the minimum

$$\min\{\int_{V'} \|p_\varphi(Df)\|_2^2 \mid f \in \mathrm{Lip}(V'), f|_{\varphi([t_0-\epsilon,t_0]\times\{\frac{-\lambda}{2}\}} = a_1 \text{ and } f|_{\varphi([t_0-\epsilon,t_0]\times\{\frac{\lambda}{2}\}} = a_2\} \quad \text{(see eq. (4))}.$$

By considering skewed Fermi coordinates as a limit case of Fermi coordinates with respect to an imaginary baseline η and by applying the calculus of variations (see [Ge], p. 14-16) to the last integral in equation (1) we obtain that f_{t_0} is given by

$$f_{t_0}(t, s) = \frac{a_2 - a_1}{H(\frac{\lambda}{2}) - H(-\frac{\lambda}{2})} H(s) + \frac{a_1 H(\frac{\lambda}{2}) - a_2 H(-\frac{\lambda}{2})}{H(\frac{\lambda}{2}) - H(-\frac{\lambda}{2})}.$$

The energy $E_{V'}(p_\varphi(DF_{t_0}))$ is

$$E_{V'}(p_\varphi(DF_{t_0})) = \frac{(a_2 - a_1)^2 \sin(\nu)|\epsilon|}{2(\arctan(\exp(\frac{\lambda}{2})) - \arctan(\exp(-\frac{\lambda}{2})))} = k_1 (a_2 - a_1)^2 |\epsilon|. \tag{24}$$

We can extend F_{t_0} to a function on V that satisfies the boundary conditions

$$F_{t_0}|_{\varphi([t_0-\epsilon,t_0]\times\{\pm x\})} = F_1|_{\varphi([t_0-\epsilon,t_0]\times\{\pm x\})}.$$

Again we choose F_{t_0}, such that it minimizes $E_{V\setminus V'}(p_\varphi(D(\cdot)))$ with the given boundary conditions. We have with $E_{V\setminus V'}(p_\varphi(DF_{t_0})) = E_{V\setminus V'}(F_{t_0})$:

$$E_{V\setminus V'}(F_{t_0}) = \frac{(a_1^2 + (1-a_2)^2)|\epsilon|}{2(\arctan(\exp(x)) - \arctan(\exp(\frac{b}{2})))} = k_2(t_0)(a_1^2 + (1-a_2)^2)|\epsilon|, \tag{25}$$

where $x = x(t_0)$ depends on t_0. For $a_1 = a_1' = F_1(p_1')$ and $a_2 = a_2' = F_1(p_2')$, we have by construction $E_V(F_1) \geq E_V(p_\varphi(DF_{t_0}))$.

Though we do not know the values a_1' and a_2', we obtain a lower bound of the energy of F_1 on V, if we determine the values $F_{t_0}(p_1') = c_1 = c_1(t_0)$ and $F_{t_0}(p_2') = c_2 = c_2(t_0)$, respectively, such that these values are minimizing the total energy $E_V(p_\varphi(F_{t_0}))$. As the two arcs γ_p^1 and γ_p^2 have the same length, we have to solve the following problem:

Find c_1, c_2, such that $1 - c_2 = c_1 \Leftrightarrow (c_2 - c_1) = 1 - 2c_1$, such that

$$E_V(p_\varphi(DF_{t_0})) = E_{V'}(p_\varphi(DF_{t_0})) + E_{V\setminus V'}(F_{t_0})$$

is minimal. We obtain from equation (24) and (25) that $c_1 = \frac{k_1}{k_2(t_0)+2k_1}$. We can cover B with a set of such strips $V_{t_0} = V$, such that these intersect only on the boundary and combine the $F_{t_0}|_{V_{t_0}}$ to a function f_1 on B. We have $E_V(F_1) \geq E_V(p_\varphi(Df_1))$.

As we consider only the energy $E_B(p_\varphi(Df_1))$ of the projection, the approximation is true in the limit case, where $\epsilon \to 0$. Due to the symmetry of the area B we obtain in total with c_1 in equation (24) and (25):

$$q_{11} = E(F_1) \geq E_B(p_\varphi(Df_1)) = 2 \int_{t=0}^{\alpha''} \frac{k_1 k_2(t)}{k_2(t) + 2k_1}\, dt. \tag{26}$$

$E_{V\setminus V'}(p_\varphi(DF_{t_0}))$ is monotonously decreasing if the length is $x - \frac{b}{2}$ increasing. Hence we find a simpler approximation for $E(F_1)$, setting $x = c$ (see (21)) in equation (25). In this case, we can set $k_2(t) = k_2(\alpha'')$ for all t. We obtain furthermore a simplified upper bound, if we define our test function only on $Z_{w'}(\alpha_2)$, where $w' = \min\{a, \frac{b}{2}\}$. This way we obtain:

$$\frac{\alpha_2}{2(\arctan(e^{w'}) - \arctan(e^{-w'}))} \geq E(F_1) = q_{11} \geq \frac{2\alpha'' k_1 k_2(\alpha'')}{k_2(\alpha'') + 2k_1}. \tag{27}$$

The lower bound that depends only on α_2, t_2 and β_1 can be obtained by expressing $\frac{b}{2}$ and λ and ν in terms of these variables (see equation (14),(22) and (23)). Using the parametrization of T_2 in equation (25) we can express the lower bound in terms of the variables α_2, t_2 and β_1. This way we obtain explicit values in equation (26).

Remark: From numerical simulations we get the impression that the lower bound for $E(F_1)$ is only usable, if the twist parameter t_2 is small. The reason for this seems to be that using the projection strongly underestimates the energy. The result gets worse with increasing t_2 and increasing length of α_2.

4.4 Summary and discussion

Let Q_i be a Q-pieces from our decompositon. We use the notation as in the previous subsections. For $j \in \{i, \tau(i), i\tau(i)\}$ let B_j be the set corresponding to $B = B_2 = B(\alpha_2)$ in the previous subsection. Let $f_{\tau(j)}$ defined on B_j analogously to the function $f_1 = f_{\tau(2)}$ on B_2 (see equation (26). Let furthermore $f_{i\tau(j)}$ on $B_{i\tau(i)}$ be the function corresponding to f_1 on B_2 which we use to obtain a lower bound for $E(\sigma_i + \sigma_{\tau(i)})$ on $S_{\alpha_{i\tau(i)}}$. We obtain the following upper and lower bounds for the entries of the matrix Q_S, where $S_i = S_{\alpha_i}$:

$$\operatorname{cap}(S_{\tau(i)} \cap Q_i) \geq q_{ii} \geq E_{B_{\tau(i)}}(p_\varphi(Df_i)).$$

Note that by definition $Q_i = Q_{\tau(i)}$ is the Q-piece containing α_i and $\alpha_{\tau(i)}$. Furthermore

$$q_{i,\tau(i)} \leq \frac{1}{2}\Big(\operatorname{cap}(S_{i,\tau(i)} \cap Q_i) - E_{B_i}(p_\varphi(Df_{\tau(i)}) - E_{B_{\tau(i)}}(p_\varphi(Df_i))\Big) \quad \text{and}$$
$$q_{i,\tau(i)} \geq \frac{1}{2}\Big(E_{B_{i,\tau(i)}}(p_\varphi(Df_{i,\tau(i)})) - \operatorname{cap}(S_i \cap Q_i) - \operatorname{cap}(S_{\tau(i)} \cap Q_i)\Big).$$

For the entries $q_{i,l}$ involving estimates from different Q-pieces Q_i and Q_l we have (see equation (10):

$$|q_{i,l}| \leq \frac{1}{2}\Big(\operatorname{cap}(S_{\tau(i)} \cap Q_i) + \operatorname{cap}(S_{\tau(l)} \cap Q_l) - E_{B_{\tau(i)}}(p_\varphi(Df_i) - E_{B_{\tau(l)}}(p_\varphi(Df_l))\Big).$$

From numerical tests we get the impression that our estimates for an entry $q_{\tau(i),\tau(i)}$ is good, if a large part of the cut locus of $CL(\alpha_i)$ is contained in Q_i and if $\alpha_i t_i$ is small. The first condition is fulfilled, if the boundary geodesic β_i is small. The estimate for q_{il} involving different Q-pieces can only be sharp, if q_{il} is small. Again, if β_i and β_l are small and if both $t_{\tau(i)}$ and $t_{\tau(l)}$ are small, we obtain a good estimate. The methods seem to work best, if all $\alpha_j, j \in \{i, \tau(i), i\tau(i)\}$ are small. This justifies the choice of α_1 in equation (11). Note that by [BSe1] it exists a canonical homology basis for a Riemann surface of genus g, where the largest element is of order g. Hence this condition can in prinpicle be satisfied for small g.

The advantage of the method is that information about the geometry of the surface can be incorporated. Suppose, for example, that the geometry of a Y-piece Y_1 attached to the Q-piece Q_1 from our decompositon is known. Then the the cut locus $CL(\alpha_2) \cap (Q_1 \cup Y_1)$ can be calculated. Incorporating this information we obtain better estimates for $E(\sigma_1)$. Information about isometries of the surface can also be incorporated. This was used in **Example 2**.

Acknowledgment

The presented work was supported the Alexander von Humboldt foundation. I would like to thank Peter Buser and Hugo Akrout for helpful discussions.

References

[Ba] Bavard, C. : *Anneaux extrémaux dans les surfaces de Riemann*, Manuscripta mathematica, **117** (2005), 265–271.

[BL] Birkenhake, Ch. and Lange, H. : *Complex Abelian varieties*, Grundlehren der mathematischen Wissenschaften (302), Springer-Verlag , Berlin Heidelberg New York, (2004).

[BMMS] Buser, P., Makover, E., Muetzel, B. and Silhol, R. : *The Jacobian of Riemann surfaces with short simple closed geodesics* (2012) (in preparation)

[BPS] Balacheff, F., Parlier H. and Sabourau, S. : *Short loop decompositions of surfaces and the geometry of Jacobians*, to appear in GAFA journal (2011).

[BS] Buser, P. and Sarnak, P. : *On the Period Matrix of a Riemann Surface of Large Genus (with an Appendix by Conway,J.H. And Sloane,N.J.A.)*, Inventiones Mathematicae **117**(1) (1994), 27–56.

[BSe1] Buser, P. and Seppälä, M. : *Short homology bases and partitions of Riemann surfaces*, Topology **41**(5) (2002), 863-871.

[BSe2] Buser, P. and Seppälä, M. : *Triangulations and homology of Riemann surfaces*, Proc. Amer. Math. Soc. **131**(2) (2003), 425-432.

[BSi] Buser, P. and Silhol, R. : *Geodesics, Periods, and equations of real hyperelliptic curves*, Duke M. J. **108** (2001), 211–250.

[Bu] Buser, P. : *Geometry and Spectra of compact Riemann surfaces*, Progress in mathematics (106), Birkhäuser Verlag, Boston, (1992).

[FK] Farkas, H.M. and Kra, I. : *Riemann Surfaces 2nd edition*, Springer-Verlag, (1992).

[Ge] Gelfand, I.M. : *Calculus of variations*, Dover Publications, New York, (2000).

[GT] Goldshtein, V. and Troyanov, M. : *Capacities in metric spaces*, Integral Equations and Operator Theory **44** (2002), 212–242.

[Hi] Hidalgo, R. A. and Figueroa, J. : *Numerical Schottky uniformizations* Geometriae Dedicata **111** (1) (2005), 125–157.

[Mu1] Muetzel, B. : *Capacities, systoles and Jacobians of Riemann surfaces*, doctorate thesis, EPFL Lausanne, (February 2011).

[Mu2] Muetzel, B. : *Inequalities for the capacity of non-contractible annuli on cylinders of constant and variable negative curvature*, submitted to Ann. Acad. Sci. Fenn. Math., (May 2011).

[Mu3] Muetzel, B. : *On the second successive minimum of the Jacobian of a Riemann surface*, to appear in Geom. Dedicata, (January 2010).

[Pa] Parlier, H. : *On the geometry of simple closed geodesics*, PhD thesis, Ecole Polytechnique Fédérale de Lausanne, (2004).

[Se] Seppala, M. : *Computation of Period Matrices of Real Algebraic-Curves*, Discrete and Computational Geometry **11**(1) (1994), 65–81.